Desalination and Water Treatment
www.deswater.com
doi: 10.1080/19443994.2016.1185743

57 (2016) 28957–28963
December

Taylor & Francis
Taylor & Francis Group

Efficient removal of methylene blue from aqueous solutions by an ordered mesoporous HPMo-SiO_2

Huawen Wang[1], Xiaofeng Peng[1], Cheng Zhou[1], Yiwei Wu*[,1]

Hubei Collaborative Innovation Center for Rare Metal Chemistry, Hubei Key Laboratory of Pollutant Analysis & Reuse Technology, College of Chemistry and Chemical Engineering, Hubei Normal University, Huangshi 435002, China, Tel. +86 071 465 15602; Fax: +86 071 465 83735; emails: whw507@163.com (H. Wang), pxfchem@163.com (X. Peng), rongyoudizhi1987@163.com (C. Zhou), chemwuyiwei@163.com (Y. Wu)

Received 9 October 2015; Accepted 29 April 2016

ABSTRACT

An ordered mesoporous HPMo-SiO_2 was synthesized and used as an adsorbent for removal of methylene blue (MB) from aqueous solutions. The morphology and structures of the material were characterized by scanning electron microscope and transmission electron microscopy. The removal process was systematically investigated under various conditions such as pH value, shaking time, the initial concentration of MB. Adsorption process was closely fitted with pseudo-second-order model and Langmuir isotherm equations. The maximum adsorption capacity for MB was 87.8 mg g^{-1} at 293 K. The results of thermodynamics studies ($\Delta G^\circ < 0$, $\Delta H^\circ > 0$, $\Delta S^\circ > 0$) showed the adsorption progress was spontaneous and endothermic. Besides, quantitative desorption of MB from HPMo-SiO_2 could be achieved with methanol containing over 25% acetic acid.

Keywords: Mesoporous HPMo-SiO_2; Methylene blue; Removal; Desorption

1. Introduction

Methylene blue (MB) (3,7-bis(dimethylamino)-phenothiazin-5-iumchloride, MB), as a cationic basic dye, is one of the most commonly used for dyeing cottons, leather, wools, and nylon in textile industries [1]. Although this dye is not strongly hazardous to humans, acute exposure to MB can cause nausea, cyanosis, gastritis, and mental confusion [2,3]. Furthermore, MB has been reported to reduce the light transmittance of water, hinder the photosynthesis, and inhibit the growth of biota [4]. Accordingly, effective measures such as coagulation [5], filtration [6], biodegradation [7] and adsorption [8–10] had been taken to remove MB from aqueous solutions. Among these techniques, adsorption is advantageous over other techniques due to being economically feasible, quick absorption, simple and fast operation, and low sensitivity to toxic substances [11–13]. Several adsorbents such as activated carbon [14], zeolites [15], agricultural byproducts [16], clays [17] and mesoporous silica [18], have been reported for removal of MB, and the ordered mesoporous silica material is a superior adsorbent due to its high stability, big surface area, large adsorption capacities, and fast absorption [19,20]. In order to improve the activity of the

*Corresponding author.

[1]Present address: Institute for Advanced Materials, Hubei Normal University, Huangshi 435002, China.

materials, some heteropoly acids [21,22] (phosphomolybdic acid and phosphotungstic acid in particular) were added into the synthetic process to change the formation of mesoporous structure. Xu et al. [23] synthesized HPMo-SiO_2 using nonionic triblock copolymer F127 (Nonionic triblock copolymer EO106PO70EO106) as a structure directing agent and tetraethyl orthosilicate (TEOS) as a silica source without doing the application experiments. Interestingly, we happened to find HPMo-SiO_2 can adsorb MB, and so far no reports of its application as adsorbent for MB removal.

In this paper, a novel, efficient and ordered mesoporous HPMo-SiO_2 was successfully synthesized and to explore its possibility for removal of MB from aqueous solutions. The removal efficiencies of MB with different factors including pH value, shaking time, and the initial concentration were investigated. And the equilibrium, kinetics, thermodynamics, and desorption were also discussed.

2. Experimental

2.1. Standard solution and reagents

MB, Methyl violet (MV), Methyl orange (MO) were purchased from Hunan Xiangzhong Chemical. The solutions of MB, MV, and MO were prepared by serial dilution of stock solution (1 mg mL^{-1}) using deionized distilled water. All chemicals in this study were of analytical grade without further purification.

A series of Britton–Robison (B–R) buffer solutions containing acetic acid, boric acid and phosphoric acid, each with a concentration of 0.04 mol L^{-1}, were used for pH adjustment. Distilled deionized water was used throughout the experiments.

2.2. Instrumentation

MB concentration was detected by a SPECORD 200 spectrometer (AnalytikJena, Jena, Germany) at 665 nm. The adsorption experiments were carried out in a shaker bath at different temperature with a THZ-C-1 refrigerated constant temperature oscillator (Taicang instrument equipment factory, Jiangsu, China). The pH values were measured with a PB-10 pH-meter (Sartorius Scientific Instruments Co., Ltd, Beijing, China). The size and shape of the HPMo-SiO_2 were determined by an S-3400N scanning electron microscope (SEM) (Hitachi, Tokyo, Japan). Transmission electron microscopy (TEM) of mesoporous HPMo-SiO_2 was performed with a Tecnai G20 transmission electron microscopy (FEI, America).

2.3. Preparation of mesoporous HPMo-SiO_2

Ordered mesoporous HPMo-SiO_2 was synthesized by a sol-gel method similar to the described procedure in the literature [23]. Briefly, 2.4 g F127 was completely dissolved in 72 mL of distilled water by vigorously stirring at room temperature, then 0.23 g HPMo (phosphomolybdic acid) was added into the solution. After the solution became homogeneous, 5.08 g TEOS (Tetraethyl orthosilicate), 0.35 g NaCl and 0.45 mL HCl (36 wt.%) were dropped into the above mixture solution in sequence. The mixture solution was stirred for 20 h at room temperature and subsequently subjected to aging at 100℃ over night. The obtained product was collected by filtration, washed with deionized water, dried at 110℃ overnight, and calcinated at 550℃ for 8 h.

2.4. General adsorption experiments

Batch adsorption experiments were carried out at 298 K in a shaker bath. In general, 0.2 g HPMo-SiO_2 was added to 100 mL of 4.0 μg mL^{-1} MB solutions at pH range 2.0–12.0. The mixture was shaken at 180 rpm for 30 min. Finally, the supernatant solution was collected and determined by the spectrophotometer.

2.5. Kinetic experiment

0.2 g HPMo-SiO_2 was mixed with 100 mL of 0.5, 2.0, 4.0 μg mL^{-1} MB at pH 7 ± 0.2, respectively. The mixtures were shaken at 180 rpm for different time intervals (5, 10, 15, 20, … 100 min) at 298 K. Finally, the supernatant solution was collected and determined by the spectrophotometer.

2.6. Sorption isotherm experiment

0.2 g HPMo-SiO_2 was mixed with 100 mL of 5.0–250.0 μg mL^{-1} MB at pH 7 ± 0.2, respectively. The mixtures were shaken at 180 rpm for 10 min at different temperature (293, 303, 313 K). Finally, the supernatant solution was collected and determined by the spectrophotometer.

3. Results and discussion

3.1. SEM and TEM image analysis

The representative morphology of HPMo-SiO_2 materials is an important factor affecting its performance and the SEM and TEM images under different magnifications are shown in Figs. 1 and 2. As seen, the SEM and TEM of HPMo-SiO_2 material displays

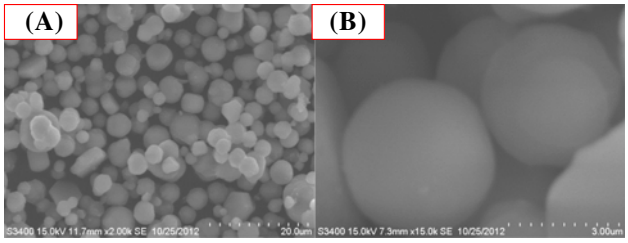

Fig. 1. SEM images of HPMo-SiO_2 at 2,000× (A) and 15,000× (B) magnifications.

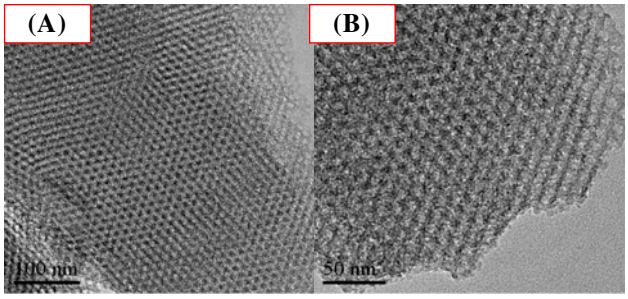

Fig. 2. TEM images of HPMo-SiO_2 at different magnifications: (A) 100 nm and (B) 50 nm.

the most ordered pore structure and the most uniform pore distribution. The diameter of the spheres is 2–3 μm, and the final pore size is around 1–1.3 nm (the unit cell parameter, i.e. distance from center of pore to center of pore, could be estimated as 1.7 nm, thus taking into account that this value (a0 = unit cell) implies pore size plus pore wall). Such structure should significantly increase the available surface area of HPMo-SiO_2, leading to improving kinetics of adsorbtion of MB and, therefore, enhancing the removal efficiency.

3.2. Selectivity of HPMo-SiO_2

A number of dyes MO, MV, and MB were tested at varying pH controlled by B–R buffer to characterize the selectivity of HPMo-SiO_2, and the results are shown in Fig. 3(A). As seen, HPMo-SiO_2 exhibits quantitative removal rate for MB at broad pH range (3.0–12.0). However, HPMo-SiO_2 can almost not remove MO and MV at pH 4.0–12.0 except for 40–60% removal rate for MO at pH 2.0–3.0. The structural formulas of MB, MV, and MO shown in Fig. 3(B) may help to explain intuitionally the excellent selectivity of HPMo-SiO_2 for MB. It may attribute to the strong electrostatic interactions between the –OH groups of the surface of HPMo-SiO_2 and the $=N^+H^-$ groups of MB. However, although MV also has the $=N^+H^-$ groups,

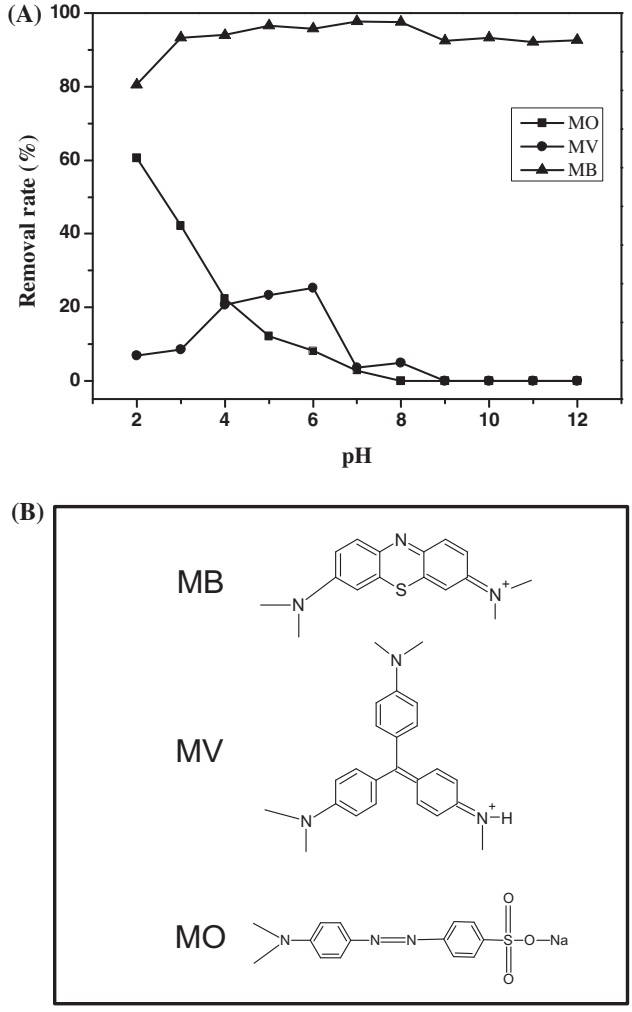

Fig. 3. (A) Effect of pH on the removal of 4.0 μg mL^{-1} MO, MV, MB by HPMo-SiO_2 and (B) the structural formulas of MB, MV, and MO.

the molecular size of MV, which is the tetrahedral structure and exists steric hindrance effect, may not match well the pore size of HPMo-SiO_2. As for MO, it is an anionic dye with negative charge $-SO_3^-$ groups, which is helpless for the electrostatic attraction between MO and HPMo-SiO_2.

3.3. Effect of adsorptive time on different initial concentration of MB

Effect of adsorptive time on different initial concentration of MB is one of the most important factors affecting the removal process. As shown in Fig. 4, with the initial concentration of MB in 2.0–4.0 μg mL^{-1}, the removal rate is over 90% at 5.0 min and keeps quantitatively at times of 5–100 min, revealing that the equilibrium is quick. While in the lower

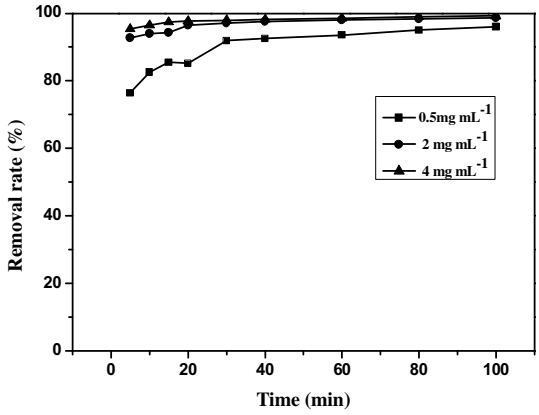

Fig. 4. Effect of adsorptive time on different initial concentration of MB (0.5, 2.0, 4.0 μg L^{-1}) at 298 K.

concentration of 0.5 μg mL^{-1}, the removal rate increases lightly with time, and the quantitative equilibration time needs 30 min. This may be owing to the mass transfer driving force which is small at low concentration.

3.4. Adsorption kinetics

To evaluate the process of adsorption, kinetics and equilibrium of adsorption are two important physical–chemical aspects. The following reaction kinetics formulas of pseudo-first-order (Eq. (1)) and pseudo-second-order (Eq. (2)) are used to analyze the adsorption kinetics data.

$$\log(q_e - q_t) = \log q_e - \frac{k_1 t}{2.303} \quad (1)$$

$$\frac{t}{q_t} = \frac{1}{k_2 q_e^2} + \frac{t}{q_e} \quad 2)$$

where q_e and q_t are the sorption capacities at equilibrium (mg g^{-1}) and at any time t (min), respectively, and k_1 (min^{-1}) is and k_2 (g mg^{-1} min^{-1}) are the constants, respectively.

The results of adsorption kinetics are calculated in Table 1 and Fig. 5. By comparing the two parameters, the calculated q_e values ($q_{e,cal}$) of the pseudo-second-order kinetic model is fitted well with the experimental ones ($q_{e,exp}$), and the plots show quite good linearity with R^2 closer to 1. Based on the values of R^2 and q_e, the adsorption kinetics follows the pseudo-second-order model well. In other words, the adsorption of MB on HPMo-SiO_2 was prevailingly controlled by the chemical process [24].

3.5. Adsorption isotherms

Langmuir isotherm (Eq. (3)) and Freundlich isotherm (Eq. (4)) were used to study the equilibrium adsorption isotherm.

$$\frac{C_e}{q_e} = \frac{1}{q_{max} K_c} + \frac{C_e}{q_{max}} \quad (3)$$

$$\ln q_e = \frac{1}{n} \ln C_e + \ln K_f \quad (4)$$

where C_e (mg L^{-1}) is the equilibrium concentration, q_e (mg g^{-1}) is the adsorption capacity at equilibrium, q_{max} (mg g^{-1}) and K_c (L mg^{-1}) are Langmuir constants related to the adsorption capacity and rate of adsorption, respectively. K_f ((mg g^{-1}) (L $mg^{-1})^{1/n}$) is roughly a Freundlich indicator of adsorption capacity, and n is adsorption intensity of Freundlich.

The Langmuir plots MB adsorption by HPMo-SiO_2 is shown in Fig. 6. The Langmuir constants (K_c and q_{max}) and Freundlich constants (K_f and n) are calculated and recorded in Table 2. As seen, the R^2 values of Langmuir and Freundlich models are 0.9950–0.9982 and 0.7882–0.8707, respectively, indicate that the adsorption equilibrium of MB onto HPMo-SiO_2 is better described by Langmuir isotherm model. The adsorption capacity of MB by HPMo-SiO_2 attains 87.8 mg g^{-1} at 293 K. Table 3 compares the adsorption capacity of different adsorbents reported for removal of MB from aqueous solutions. It is obvious that

Table 1
Adsorption kinetics of MB

Initial concentration of MB (μg mL^{-1})	$q_{e,exp}$ (mg g^{-1})	Pseudo-first-order kinetic parameters			Pseudo-second-order kinetic parameters		
		k_1	$q_{e,cal}$ (mg g^{-1})	R^2	k_2	$q_{e,cal}$ (mg g^{-1})	R^2
0.5	0.1784	0.01432	69.8432	0.9292	5.5855	0.1790	0.9997
2	0.8913	0.01615	61.9195	0.9604	1.1195	0.8933	0.9999
4	1.7406	0.01333	75.0187	0.9415	0.5749	1.7406	0.9999

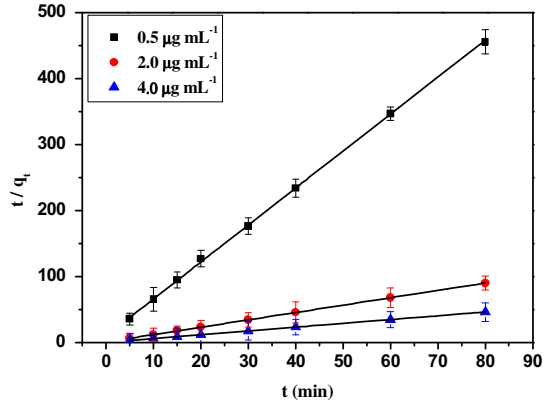

Fig. 5. Pseudo-second-order adsorption kinetics on HPMo-SiO_2.

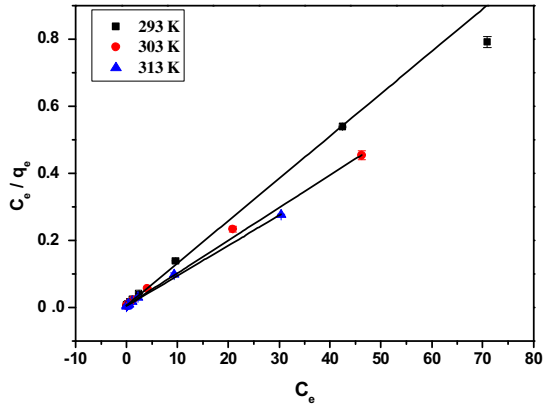

Fig. 6. Langmuir isotherm of MB adsorption by HPMo-SiO_2.

adsorption capacity of HPMo-SiO_2 is higher than that of works [25–29,31] and a little less than that [30].

3.6. Thermodynamic study

The thermodynamic parameters were studied at the temperature (293, 303, 313 K) to reveal the inherent energetic changes in adsorption process, such as Gibbs free energy (ΔG°, kJ mol^{-1}), enthalpy change (ΔH°, kJ mol^{-1}) and entropy change (ΔS°, J mol^{-1} K^{-1}). Then, they can be calculated by the following formulas:

$$\Delta G^\circ = -RT \ln K_L \quad (5)$$

$$\ln K_L = \frac{\Delta S^\circ}{R} - \frac{\Delta H^\circ}{RT} \quad (6)$$

where R is universal gas constant (8.314 J mol^{-1} K^{-1}) and T is the temperature (K). K_L is thermodynamic equilibrium constant calculated from Eq. (3).

The results are listed in Table 4. From Table 4, ΔG° are between –0.5690 and –3.3478 kJ mol^{-1}, indicating the present adsorption reaction of MB on HPMo-SiO_2 was spontaneous. The positive value of ΔH° demonstrates the endothermic character of MB adsorption on HPMo-SiO_2, and the positive value of ΔS° suggests the increased randomness at solid/solution interface during the adsorption process.

3.7. Effect of ionic strength

Since real time waste water contains salts, it is important to study the ability of adsorbent for removal of MB in presence of ionic salts. Effect of NaCl ranging from 0.1 to 0.5 mol L^{-1} on the adsorption of MB onto HPMo-SiO_2 was examined. The results indicated that the removal rate of MB had no obvious affects with the varying concentrations of NaCl.

3.8. Desorption of MB from HPMo-SiO_2

In order to desorb MB from HPMo-SiO_2, different volume ratios (0:5, 1:4, 2:3, 3:2, 4:1, 5:0) of acetic acid to methanol were carried out. The results showed that MB could be completely desorbed with 1:4, 2:3, 3:2, 4:1, 5:0 volume ratios of acetic acid to methanol only except for 0:5. According to the phenomenon, it can be deduced that acetic acid may damage the strong electrostatic interactions of between the –OH groups

Table 2
Isotherm parameters for MB adsorption by HPMo-SiO_2

	Langmuir			Freundlich		
Temperature (K)	q_{max} (mg g^{-1})	K_c	R^2	$1/n$	K_f	R^2
293	87.8	0.925	0.9950	0.36	30.38	0.7882
303	101.73	1.108	0.9967	0.41	36.95	0.8256
313	111.48	1.355	0.9982	0.44	43.96	0.8707

Table 3
Comparison of the adsorption capacities of MB onto various adsorbents

Adsorbents	Maximum adsorption capacities (mg g^{-1})	Refs.
Activated carbon-coated palygorskite	351	[14]
AlMCM-41	66.53	[25]
Highly-ordered mesoporous SBA-15	49.26	[26]
Multi-walled carbon nanotubes filled with Fe_2O_3 particles	42.3	[27]
$ZnCo_2O_4$ microspheres	79.1	[28]
Carbon nanotubes	35	[29]
PDA microspheres	90.7	[30]
Mesoporous Fe_3O_4@SiO_2	33.12	[31]
Bamboo-based activated carbon	454.20	[32]
Activated carbon	404.089	[33]
HPMo-SiO_2	87.8	This work

Table 4
Thermodynamic parameters

Temperature (K)	ΔG° (kJ mol^{-1})	ΔS° (J mol^{-1} K^{-1})	ΔH° (kJ mol^{-1})
293	−0.5690	139.0114	40.1719
303	−1.9912		
313	−3.3478		

of the surface of HPMo-SiO_2 and the $=N^+H^-$ groups of MB since the acidity of acetic acid has changed the electric charge of the surface of HPMo-SiO_2.

4. Conclusions

In this study, HPMo-SiO_2 was prepared and employed to remove MB from aqueous solutions. HPMo-SiO_2 showed excellent selectivity towards MB at broad pH 3.0–12.0, high adsorption capacity (87.8 mg g^{-1}) and quick quantitative equilibrium time (5.0 min at over 2.0 μg mL^{-1} MB). Adsorption equilibrium process was better described by pseudo-second-order model and Langmuir isotherm. Thermodynamics studies ($\Delta G^\circ < 0$, $\Delta H^\circ > 0$, $\Delta S^\circ > 0$) suggests the adsorption process is spontaneous and endothermic in nature, and quantitative desorption of MB from HPMo-SiO_2 could be achieved with methanol containing over 25% acetic acid. All of these results suggest that HPMo-SiO_2 is a promising and efficient adsorbent for removal of MB from aqueous solutions.

Acknowledgments

This project was financially supported by Education Committee of Hubei Province (D20132501), Hubei Key Laboratory of Pollutant Analysis and Reuse Technique (Hubei Normal University) (KL2013M06).

References

[1] R. Suresh, K. Giribabu, R. Manigandan, S. Munusamy, S.P. Kumar, S. Muthamizh, A. Stephen, V. Narayanan, Doping of Co into V_2O_5 nanoparticles enhances photodegradation of methylene blue, J. Alloys Compd. 598 (2014) 151–160.
[2] M. Ghaedi, N. Zeinali, A.M. Ghaedi, M. Teimuori, J. Tashkhourian, Artificial neural network-genetic algorithm based optimization for the adsorption of methylene blue and brilliant green from aqueous solution by graphite oxide nanoparticle, Spectrochim. Acta Part A 125 (2014) 264–277.
[3] T.K. Sen, S. Afroze, H.M. Ang, Equilibrium, kinetics and mechanism of removal of methylene blue from aqueous solution by adsorption onto pine cone biomass of pinus radiata, Water Air Soil Pollut. 218 (2011) 499–515.
[4] R.P. Han, Y. Wang, X. Zhao, Y.F. Wang, F.L. Xie, J.M. Cheng, M.S. Tang, Adsorption of methylene blue by phoenix tree leaf powder in a fixed-bed column: Experiments and prediction of breakthrough curves, Desalination 245 (2009) 284–297.
[5] C.S.D. Rodrigues, L.M. Madeira, R.A.R. Boaventura, Treatment of textile dye wastewaters using ferrous sulphate in a chemical coagulation/flocculation process, Environ. Technol. 34 (2013) 719–729.
[6] S. Mondal, H. Ouni, M. Dhahbi, S. De, Kinetic modeling for dye removal using polyelectrolyte enhanced ultrafiltration, J. Hazard. Mater. 229–230 (2012) 381–389.
[7] M. Cheng, G.M. Zeng, D.L. Huang, C. Lai, Z. Wei, N.J. Li, P. Xu, C. Zhang, Y. Zhu, X.X. He, Combined biological removal of methylene blue from aqueous solutions using rice straw and Phanerochaete chrysosporium, Appl. Environ. Microbiol. 99 (2015) 5247–5256.

[8] J.F. Ma, D.Q. Huang, J. Zou, L.Y. Li, Y. Kong, S. Komarneni, Adsorption of methylene blue and Orange II pollutants on activated carbon prepared from banana peel, J. Porous Mater. 22 (2015) 301–311.
[9] K. Mahmoudi, K. Hosni, N. Hamdi, E. Srasra, Kinetics and equilibrium studies on removal of methylene blue and methyl orange by adsorption onto activated carbon prepared from date pits-A comparative study, Korean J. Chem. Eng. 32 (2015) 274–283.
[10] X.X. Liu, J. Luo, Y.T. Zhu, Y. Yang, S.J. Yang, Removal of methylene blue from aqueous solutions by an adsorbent based on metal-organic framework and polyoxometalate, J. Alloys Compd. 648 (2015) 986–993.
[11] A. Aluigi, F. Rombaldoni, C. Tonetti, L. Jannoke, Study of Methylene Blue adsorption on keratin nanofibrous membranes, J. Hazard. Mater. 268 (2014) 156–165.
[12] F. Liu, S. Chung, G. Oh, T.S. Seo, Three-dimensional graphene oxide nanostructure for fast and efficient water-soluble dye removal, ACS Appl. Mater. Interfaces 4 (2012) 922–927.
[13] H. Karimi, M. Ghaedi, Application of artificial neural network and genetic algorithm to modeling and optimization of removal of methylene blue using activated carbon, J. Ind. Eng. Chem. 20 (2014) 2471–2476.
[14] X.L. Zhang, L.P. Cheng, X.P. Wu, Y.Z. Tang, Y.C. Wu, Activated carbon coated palygorskite as adsorbent by activation and its adsorption for methylene blue, J. Environ. Sci. 33 (2015) 97–105.
[15] C.X. Li, H. Zhong, S. Wang, J.R. Xue, Z.Y. Zhang, Removal of basic dye (methylene blue) from aqueous solution using zeolite synthesized from electrolytic manganese residue, J. Ind. Eng. Chem. 23 (2015) 344–352.
[16] L.Y. Kong, L. Gong, J.Q. Wang, Removal of methylene blue from wastewater using fallen leaves as an adsorbent, Desalin. Water Treat. 53 (2015) 2489–2500.
[17] L. Cottet, C.A.P. Almeida, N. Naidek, M.F. Viante, M.C. Lopes, N.A. Debacher, Adsorption characteristics of montmorillonite clay modified with iron oxide with respect to methylene blue in aqueous media, Appl. Clay Sci. 95 (2014) 25–31.
[18] X.C. Xiao, F. Zhang, Z.P. Feng, S.J. Deng, Y.D. Wang, Adsorptive removal and kinetics of methylene blue from aqueous solution using NiO/MCM-41 composite, Physica E 65 (2015) 4–12.
[19] S. Rashi, S.K. Prajapati, D. Singh, Mesoporous silica nanoparticles for controlled drug delivery, J. Pharm. Sci. 4 (2015) 332–347.
[20] J.S. Beck, J.C. Vartuli, W.J. Roth, M.E. Leonowicz, C.T. Kresge, K.D. Schmitt, C.T.W. Chu, D.H. Olson, E.W. Sheppard, S.B. McCullen, J.B. Higgins, J.L. Schlenker, A new family of mesoporous molecular sieves prepared with liquid crystal templates, J. Am. Chem. Soc. 114 (1992) 10834–10843.
[21] R. Jorge, G.A. Aida, S.M. Felipe, V. Macías-Alcántara, P. Castillo-Villalón, L. Oliviero, F. Maugé, HDS of 4.6-DMDBT over NiMoP/(x)Ti-SBA-15 catalysts prepared with H3PMo12O40, Energ, Fuel 26 (2012) 773–782.
[22] X.L. Sheng, Y.M. Zhou, Y.W. Zhang, Y.Z. Duan, Z.W. Zhang, Y.L. Yang, Immobilization of 12-Tungstophosphoric acid in alumina-grafted mesoporous LaSBA-15 and its catalytic activity for alkylation of o-xylene with styrene, Microporous Mesoporous Mater. 161 (2012) 25–32.
[23] S.W. Xu, H.P. Pu, H. Wang, C.Y. Han, D. Dongquan, Y.Y. Zhang, Y.M. Luo, A facile route for rapid synthesis of cubic mesoporous silica, J. Phys. Chem. 73 (2012) 1252–1258.
[24] Y. Li, H.N. Xiao, M.D. Chen, Z.P. Song, Y. Zhao, Absorbents based on maleic anhydride-modified cellulose fibers/diatomite for dye removal, J. Mater. Sci. 49 (2014) 6696–6704.
[25] S. Eftekhari, A. Habibi-Yangjeh, S. Sohrabnezhad, Application of AlMCM-41 for competitive adsorption of methylene blue and rhodamine B: Thermodynamic and kinetic studies, J. Hazard. Mater. 178 (2010) 349–355.
[26] C.H. Huang, K.P. Chang, H.D. Ou, Y.C. Chiang, E.E. Chang, C.F. Wang, Characterization and application of Ti-containing mesoporous silica for dye removal with synergistic effect of coupled adsorption and photocatalytic oxidation, J. Hazard. Mater. 186 (2011) 1174–1182.
[27] S. Qu, F. Huang, S.N. Yu, G. Chen, J.L. Kong, Magnetic removal of dyes from aqueous solution using multi-walled carbon nanotubes filled with Fe_2O_3 particles, J. Hazard. Mater. 160 (2008) 643–647.
[28] H.X. Guo, J.H. Chen, W. Weng, Q.X. Wang, S.X. Li, Facile template-free one-pot fabrication of $ZnCo_2O_4$ microspheres with enhanced photocatalytic activities under visible-lightillumination, Chem. Eng. J. 239 (2014) 192–199.
[29] Y.J. Yao, F.F. Xu, M. Chen, Z.X. Xu, Z.W. Zhu, Adsorption behavior of methylene blue on carbon nanotubes, Bioresour. Technol. 101 (2010) 3040–3046.
[30] X.J. Tan, L.J. Lu, L.Z. Wang, J.L. Zhang, Facile synthesis of bimodal mesoporous Fe_3O_4@SiO_2 composite for efficient removal of methylene blue, Eur. J. Inorg. Chem. 2015 (2015) 2928–2933.
[31] J.W. Fu, Z.H. Chen, M.H. Wang, S.J. Liu, J.H. Zhang, J.N. Zhang, R.P. Han, Q. Xu, Adsorption of methylene blue by a high-efficiency adsorbent (polydopamine microspheres): Kinetics, isotherm, thermodynamics and mechanism analysis, Chem. Eng. J. 259 (2015) 53–61.
[32] B.H. Hameed, A.T.M. Din, A.L. Ahmad, Adsorption of methylene blue onto bamboo-based activated carbon: Kinetics and equilibrium studies, J. Hazard. Mater. 141 (2007) 819–825.
[33] B. Djahed, E. Shahsavani, F.K. Naji, A.H. Mahvi, A novel and inexpensive method for producing activated carbon from waste polyethylene terephthalate bottles and using it to remove methylene blue dye from aqueous solution, Desalin. Water Treat. 57 (2016) 9871–9880.